Journal of Non-Crystalline Solids 481 (2018) 282–288

Contents lists available at ScienceDirect

Journal of Non-Crystalline Solids

journal homepage: www.elsevier.com/locate/jnoncrysol

Letter to the editor

Structure of $BaO-TeO_2$ glasses: A two-dimensional ^{125}Te NMR spectroscopic study

Zachary Whittles[a], Maxwell Marple[a], Ivan Hung[b], Zhehong Gan[b], Sabyasachi Sen[a,*]

[a] Dept. of Materials Science & Engineering, University of California, Davis, CA 95616, USA
[b] Center of Interdisciplinary Magnetic Resonance, National High Magnetic Field Laboratory, 1800 East Paul Dirac Drive, Tallahassee, FL 32310, USA

ARTICLE INFO

Keywords:
125Te pjMATPASS NMR spectroscopy
$BaO-TeO_2$ glass
Tellurite
Structure

ABSTRACT

The compositional evolution of the network structure of binary $(BaO)_x(TeO_2)_{100-x}$ glasses ($5 \le x \le 25$) is studied using two-dimensional ^{125}Te isotropic-anisotropic correlation nuclear magnetic resonance (NMR) spectroscopy. It is demonstrated that only a consideration of the full ^{125}Te chemical shift tensor in combination with the composition dependent evolution of isotropic ^{125}Te NMR line shape can yield a consistent structural model of these glasses in terms of the complex tellurium speciation. When taken together, the results indicate that the addition of the modifier BaO results in a progressive depolymerization of the network of corner- and edge-shared $TeO_{4/2}$ trigonal bipyramids via their replacement with primarily a combination of negatively charged $TeO_{3/2}O$ trigonal bipyramids and $TeO_{1/2}O_2$ trigonal pyramids with one and two non-bridging oxygen, respectively.

1. Introduction

Relatively wide glass formation ranges have been reported for binary alkali and alkaline-earth and transition metal tellurites [1]. These glasses have received significant attention owing to their large optical nonlinearity, infrared transparency, high refractive index, relatively low melting point and good chemical and thermal stability [1]. Additionally, semiconducting properties have also been investigated for switching applications in glasses in the $V_2O_5-TeO_2$ system [1,2]. Although the structure of these glasses is characterized by a Te-O-Te network, pure TeO_2 itself is a conditional glass-former which requires fast quenching for glass formation [3]. The structure of these glasses and, in particular, that of alkali tellurites, has been studied in the past using a variety of spectroscopic and diffraction techniques [3–8]. However, the complexity of the Te-O coordination environments has made an unequivocal interpretation of the structural data extremely challenging. This complexity can be appreciated by considering the range of Te-O polyhedral units that are known to be present in the crystal structures of alkali tellurites which have been denoted by McLaughlin et al. using the Q_n^m notation system [3]. In this notation system, n is the coordination number of the central Te atom, i.e., the number of nearest neighbor oxygen atoms and m represents the number of bridging oxygen and hence, $m \le n$. Consequently, each of these Q species carries (n - m) non-bridging oxygen (NBO) atoms.

A total of five different types of Te species are found in alkali tellurite crystals (Fig. 1), two of which are fourfold coordinated (trigonal bipyramids): Q_4^4 and Q_4^3, and three are threefold coordinated (trigonal pyramids): Q_3^2, Q_3^1 and Q_3^0 [3,7,9–11]. It may be noted here that the "Q" in the "Q species" notation stems from "quaternary", meaning four bonds. Therefore, one should use a separate notation for threefold coordinated Te species. However, here we use the Q_n^m notation system for both fourfold and threefold coordinated Te species in order to be consistent with previous literature [3]. The wide variety of Te-O coordination environments in tellurites are impossible to distinguish in the radial distribution functions of glasses derived from the X-ray or neutron diffraction data [3,4]. On the other hand, the structural assignment of the vibrational bands in the Raman spectra remains controversial and the problem is further compounded by the fact that such spectra are not quantitative without the knowledge of the scattering cross sections of these bands. In contrast, element specific structural probes such as nuclear magnetic resonance (NMR) spectroscopy are sensitive to both the coordination number and geometry of the environment of an atom. To this end, Sakida and coworkers utilized ^{125}Te NMR spectroscopy to establish the chemical shift systematics of a wide variety of tellurite crystals and produced a map of the chemical shift anisotropy (CSA) Δ vs. the asymmetry parameter η for the various species [10]. It may be noted here that if the principal components of the ^{125}Te chemical shift tensor are δ_{xx}, δ_{yy}, and δ_{zz}, then the tensor is completely defined by the parameters [12]:

isotropic shift $\delta_{iso} = \frac{1}{3}(\delta_{zz} + \delta_{xx} + \delta_{yy})$,

* Corresponding author.
E-mail address: sbsen@ucdavis.edu (S. Sen).

https://doi.org/10.1016/j.jnoncrysol.2017.10.055
Received 15 September 2017; Received in revised form 24 October 2017; Accepted 29 October 2017
Available online 14 November 2017

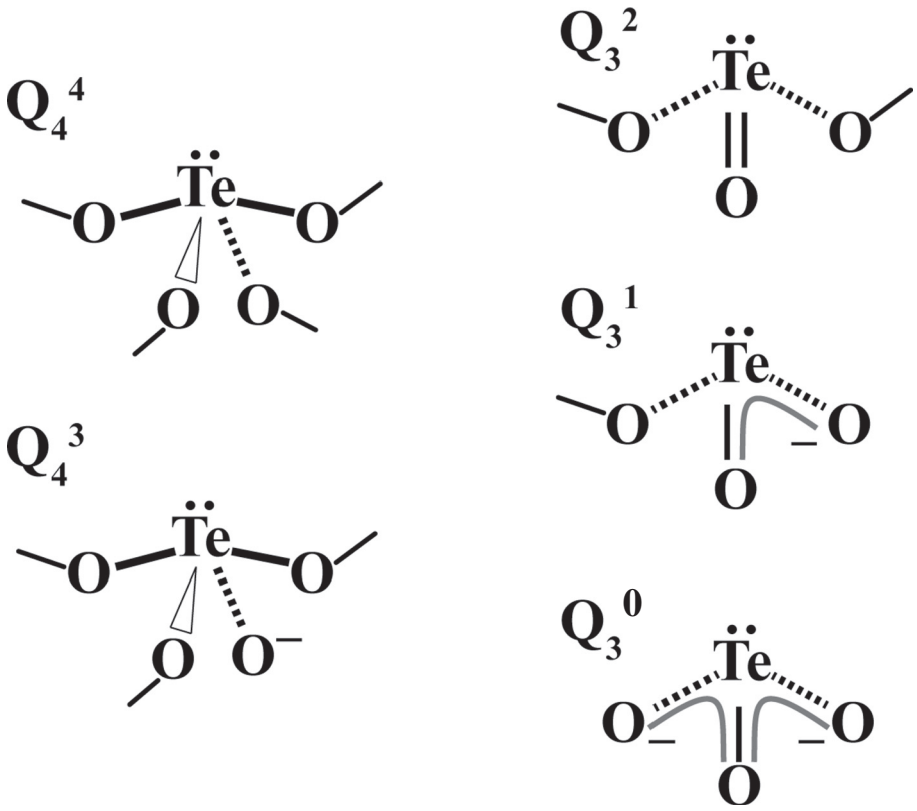

Fig. 1. Cartoon representation of Te coordination environments found in alkali tellurite crystals and their Q-species nomenclature [3].

$$\Delta = \frac{3}{2}(\delta_{zz} - \delta_{iso}),$$

$$\eta = \frac{\delta_{yy} - \delta_{xx}}{\delta_{zz} - \delta_{iso}},$$

Here, by convention: $\delta_{zz} - \delta_{iso} \geq \delta_{xx} - \delta_{iso} \geq \delta_{yy} - \delta_{iso}$.

The Δ vs. η map of Sakida et al. [10] appears to define separate regions for the various Q_n^m units and thereby promises to be an effective tool for identification of such units in glasses. However, the chemical shift range of a nuclide such as ^{125}Te is enormous (several hundreds of ppm in tellurites) and thus, the typical one-dimensional ^{125}Te NMR spectra of tellurite glasses are broadened by a combination of chemical shift distribution and large CSA to an extent that makes it practically impossible to separate the contributions from different Q_n^m units. In contrast to one-dimensional NMR, the two-dimensional Magic-Angle Turning Phase-Adjusted Sideband Separation (2D MATPASS) spectroscopic technique separates the CSA from the isotropic chemical shift, resulting in increased spectral resolution while preserving the information contained in the CSA [12–14]. Correlation of the CSA and isotropic dimensions can provide unequivocal identification of various structural units. Moreover, the application of Carr-Purcell-Meiboom-Gill (CPMG) echo train acquisition of the MATPASS data drastically reduces the experimental time such that a high-resolution spectrum for low natural abundance nuclides such as ^{125}Te (~7%) can be acquired within a reasonable timespan.

In the present study, instead of the MATPASS/CPMG NMR, the projection MATPASS/CPMG (*pj*MATPASS/CPMG) NMR spectroscopy is utilized to study the structure of $(BaO)_x(TeO_2)_{100-x}$ glasses with $5 \leq x \leq 25$. The *pj*MATPASS/CPMG NMR provides identical information as the MATPASS/CPMG technique described above, but uses projection pulses to cover a large chemical shift range [15], making it an ideal sequence for high-field ^{125}Te NMR in glasses [12]. We report the details of a self-consistent analysis of the isotropic and anisotropic ^{125}Te NMR spectra of these glasses, which yields a reasonable model of the composition dependent evolution of the Te-O network for these glasses.

2. Experimental

2.1. Sample synthesis and physical characterization

A total of Five $(BaO)_x(TeO_2)_{100-x}$ glasses with x = 5,10,15,20 and 25 were synthesized in 5 g batches from 99.9% pure TeO_2 and $BaCO_3$ (Alfa) precursors in Pt-Au crucibles via the conventional melt-quench method. The batches were melted for 30 min at 750 °C–850 °C and quenched by dipping the bottom of the crucible in cold water. The chemical composition of the resulting glasses was analyzed using a Cameca SE-100 electron microprobe equipped with wavelength dispersive spectrometers and was found to be within 0.5 mol% of the nominal composition. Conventional differential scanning calorimetric (DSC) scans of these glasses were taken using a Mettler-Toledo DSC1 calorimeter to determine the glass transition temperature T_g, which was taken as the onset of the glass transition region when heating at a rate of 10 K/min. The DSC scans were performed in a flowing nitrogen environment on 15–20 mg of sample loaded into 40 μL aluminum crucibles. Density measurements were carried out using a Micromeritics AccuPyc II gas expansion pycnometer under a helium environment of 6 N purity. Approximately 2.0 g of each sample was loaded into a 1 cm^3 cup. Reported densities are averages of 10 consecutive measurements at 20 °C. Samples were not annealed before the density measurement.

2.2. ^{125}Te *pj*MATPASS/CPMG NMR spectroscopy

All ^{125}Te NMR measurements were carried out at the National High Magnetic Field Laboratory (NHMFL) on a 31 mm bore 19.6 T magnet equipped with a Bruker DRX console, operating at a resonance frequency of 262.8 MHz for ^{125}Te. Crushed glass samples were spun at 10 kHz in ZrO_2 rotors with a 3.2 mm HX Low-E MAS probe designed and built at the NHMFL. The *pj*MATPASS/CPMG NMR pulse sequence is described in detail in a previous work [12]. The ^{125}Te 2D *pj*MATPASS/CPMG spectra of the glass samples were each acquired using 16 hypercomplex t_1 data points with 24 transients per point, 86 CPMG echoes

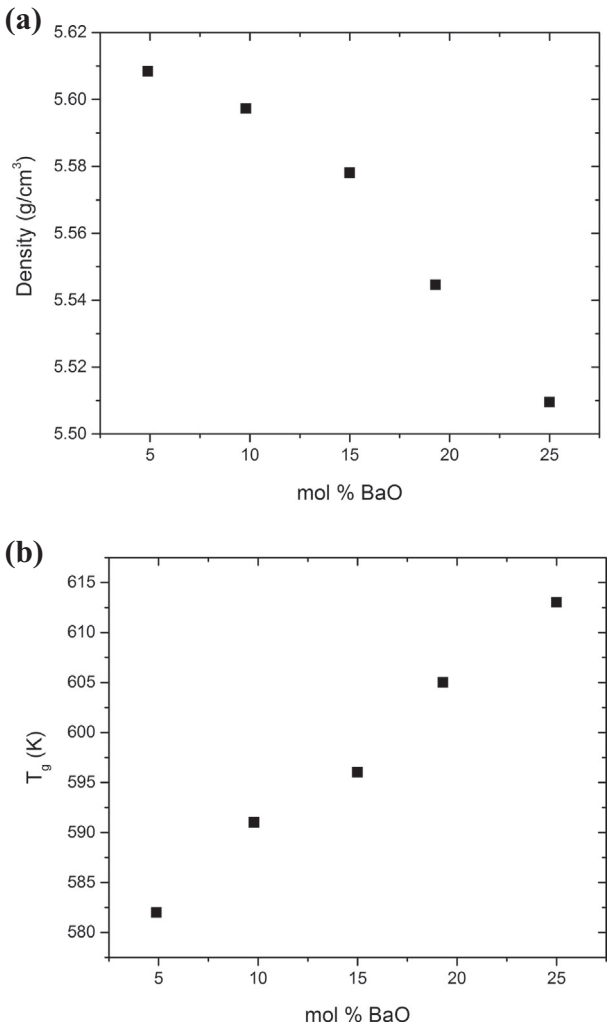

Fig. 2. Compositional variation of (a) density and (b) T_g of BaO-TeO_2 glasses.

per transient and a recycle delay of 50 s. A 2.5 μs duration was used for *all pulses* in the *pj*MATPASS/CPMG pulse sequence. All spectra were referenced to neat $(CH_3)_2Te$ with δ_{iso} at 0 ppm by measuring the ^{17}O resonance frequency of tap water and using the frequency ratios between ^{17}O and ^{125}Te reported in the IUPAC recommendations [16]. The 2D isotropic-CSA correlation spectra were obtained by the summation of the CPMG echoes, Fourier transformation along both dimensions and shearing of the direct F_2 dimension. The projections along the isotropic and the anisotropic dimensions were simulated using DMfit [17].

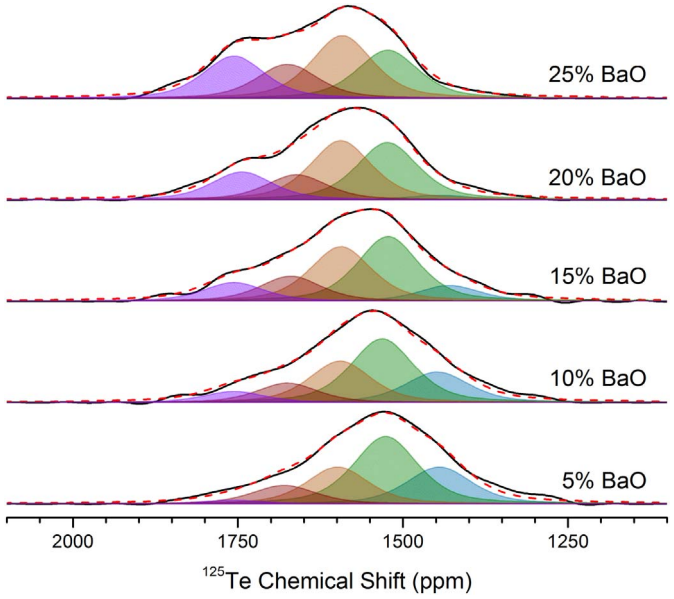

Fig. 4. Experimental (solid black lines) and simulated (dashed red lines) isotropic ^{125}Te NMR spectra of $(BaO)_x(TeO_2)_{100-x}$ glasses. Individual simulation components are also shown. Glass compositions are denoted alongside the spectra. (For interpretation of the references to color in this figure legend, the reader is referred to the web version of this article.)

3. Results and discussion

The composition dependence of the density and the T_g of the $(BaO)_x(TeO_2)_{100-x}$ glasses determined in this study is shown in Fig. 2. The density decreases and T_g increases monotonically with increasing BaO content, although the ranges of variation of these quantities are rather small compared to those observed in other simply modified binary oxide glasses. These results are in good agreement with those reported in previous studies on glasses in this system [18,19]. Since the structural evolution of tellurite glasses still remains a rather controversial subject, here we do not attempt to establish the structure-property relationship but rather focus, in what follows, on building a structural model for these Ba-tellurite glasses, based on the ^{125}Te NMR spectroscopic data.

A representative 2D ^{125}Te *pj*MATPASS/CPMG NMR spectrum of one of the $(BaO)_x(TeO_2)_{100-x}$ glasses studied here is shown in Fig. 3. As

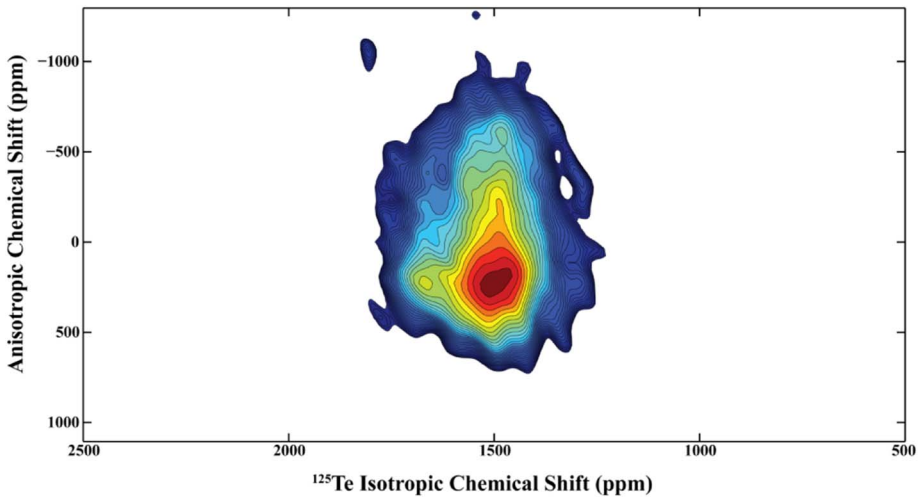

Fig. 3. Contour plot of 2D ^{125}Te *pj*MATPASS/CPMG NMR spectrum of $(BaO)_{20}(TeO_2)_{80}$ glass.

Table 1
Simulation parameters for ^{125}Te *pj*MATPASS/CPMG isotropic line shapes.

Glass composition	Te-O coordination environment	Position (ppm)	Width (ppm)	Relative fraction (%)
5%BaO – 95%TeO_2	Q_4^4	1445	115	23
	Q_4^4	1526	115	42
	Q_4^3	1599	110	22
	Q_3^2	1680	115	11
	Q_3^1	1756	110	2
10%BaO – 90%TeO_2	Q_4^4	1448	115	19
	Q_4^4	1531	113	39
	Q_4^3	1595	110	24
	Q_3^2	1675	110	11
	Q_3^1	1756	110	7
15%BaO – 85%TeO_2	Q_4^4	1430	110	9
	Q_4^4	1523	110	36
	Q_4^3	1594	110	31
	Q_3^2	1670	110	14
	Q_3^1	1756	110	10
20%BaO – 80%TeO_2	Q_4^4	1445	110	3
	Q_4^4	1523	110	33
	Q_4^3	1594	110	34
	Q_3^2	1661	110	14
	Q_3^1	1744	110	16
25%BaO – 75%TeO_2	Q_4^4	1445	110	0
	Q_4^4	1523	110	26
	Q_4^3	1592	110	33
	Q_3^2	1675	110	18
	Q_3^1	1756	110	23

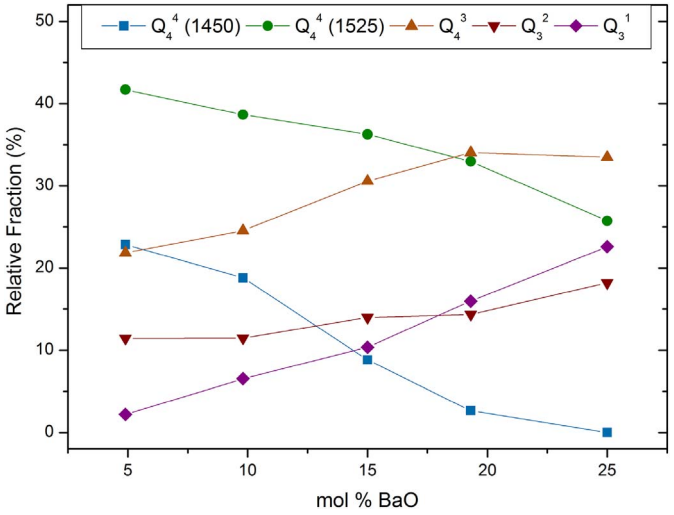

Fig. 5. Compositional variation of relative fractions of various tellurium Q species derived from ^{125}Te NMR. Solid lines through the data points are guides to the eye.

noted above, the projection of such a spectrum along the isotropic dimension is only broadened by the chemical shift distribution and corresponds effectively to a magic-angle-spinning (MAS) spectrum collected at "infinite" spinning speed. On the other hand, the slices of this spectrum in the anisotropic dimension provide information regarding the ^{125}Te chemical shift anisotropy. The isotropic ^{125}Te NMR spectra of these glasses are shown in Fig. 4, which clearly display an increase in relative intensity on the high frequency (high ppm) side with increasing BaO content. Simulation of these line shapes with multiple peaks at specific positions and with uniform full-width-at-half maximum (FWHM) requires five mixed Gaussian-Lorentzian (50% Gaussian) components centered at δ_{iso} ~1450, 1530, 1600, 1675 and 1755 ppm with FWHM ~110 ppm (Fig. 4). The center frequencies of the five

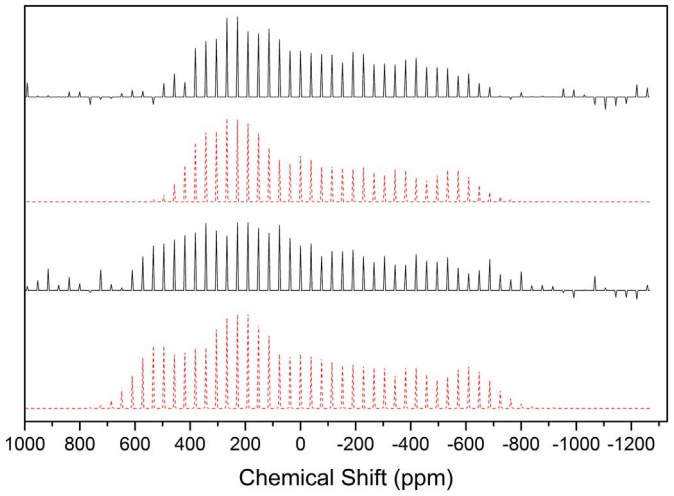

Fig. 6. Comparison of the experimental (solid black line) and simulated (dashed red line) anisotropic ^{125}Te NMR sideband spikelet patterns of $(BaO)_{20}(TeO_2)_{80}$ glass, taken at δ_{iso} = 1700 ppm (top) and at δ_{iso} = 1450 ppm (bottom). (For interpretation of the references to color in this figure legend, the reader is referred to the web version of this article.)

components and their fixed FWHM were optimized by simultaneous fitting of all isotropic ^{125}Te NMR line shapes in Fig. 4 using an iterative procedure with DMfit. The corresponding simulation parameters are listed in Table 1 and the compositional variation of the relative areas/fractions of these component peaks are shown in Fig. 5. Although such simulations are non-unique and the structural assignments of these five components are not known a priori, as shown below, careful consideration of the compositional variation of their relative fractions in combination with their chemical shift anisotropy and asymmetry parameters yield a self-consistent model of the structural evolution of these glasses.

First of all, it is clear from Fig. 4 and Table 1 that, with increasing BaO content, the peaks at 1675 and 1755 ppm grow at the expense of the peaks at 1450 and 1530 ppm. Further analysis requires consideration of the chemical shift tensor for these peaks. To this end, the spinning sideband intensities from the anisotropic dimension of the 2D ^{125}Te *pj*MATPASS/CPMG NMR spectra at various δ_{iso} values were simulated using the Herzfeld-Berger method in DMFit (Fig. 6) to obtain the variation in Δ and η as a function of δ_{iso}, for all glass compositions (Fig. 7). It is important to note in Fig. 7 that both $|\Delta|$ and η change significantly in the range of δ_{iso} ~1600 ppm. Moreover, the $|\Delta|$ and η values for the five components at their respective peak positions are shown in Fig. 8 along with the ^{125}Te chemical shift tensor systematics, as established by Sakida et al. for a wide variety of tellurite crystals [10]. It is clear from Fig. 8 that the Q_3^m Te species are in general characterized by lower $|\Delta|$ and η, compared to the Q_4^m species. Therefore, when taken together, the observed variation in $|\Delta|$ and η with δ_{iso} for the $(BaO)_x(TeO_2)_{100-x}$ glasses in Figs. 7 and 8 suggests that the two components with δ_{iso} = 1675 ppm and 1755 ppm must belong to the Q_3^m species, consistent with the increase in their relative abundance with increasing BaO (Fig. 5, Table 1). Furthermore, the $|\Delta|$ values in this region always stay higher than 1000 ppm (Fig. 7), which precludes the existence of any significant fraction of Q_3^0 species in these glasses as such species are characterized by $|\Delta|$ values smaller than 750 ppm (Fig. 8). These results, in conjunction with fact that the ratio of the relative fractions of the peaks at 1675 ppm and 1755 ppm decrease with increasing BaO content (Fig. 5, Table 1), suggest that it is reasonable to assign them to Q_3^2 and Q_3^1 species, respectively. On the other hand, the peaks centered at 1450 ppm and 1530 ppm are characterized by δ_{iso}, $|\Delta|$ and η values that are quite similar to those reported for the Q_4^4 species in tellurites. This structural assignment is also consistent with the progressive lowering of the relative fractions of

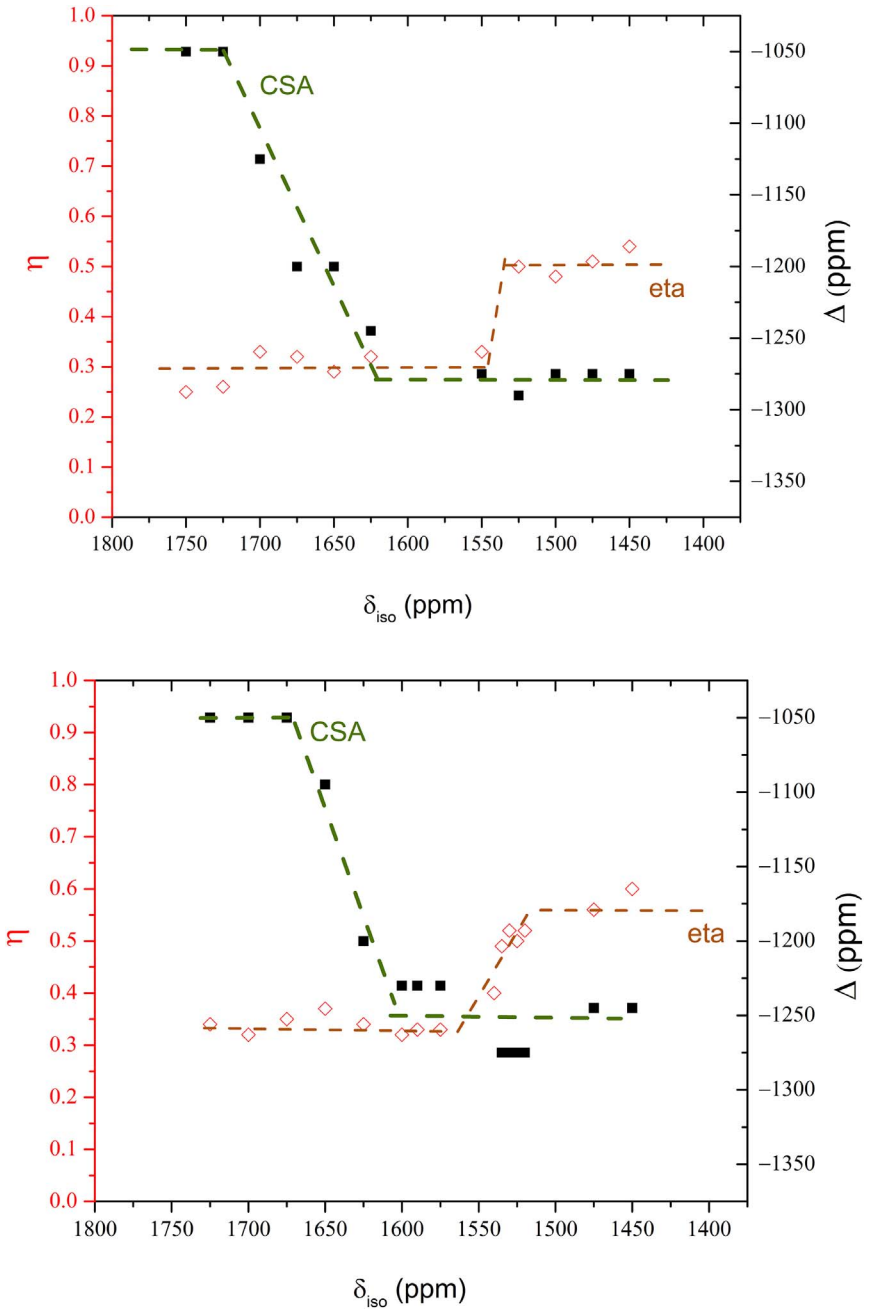

Fig. 7. Representative variation in Δ (filled symbols) and η (open symbols) as a function of δ_{iso} for $(BaO)_{10}(TeO_2)_{90}$ (top) and $(BaO)_{20}(TeO_2)_{80}$ (bottom) glasses. Dashed lines through the data points are guides to the eye.

these two peaks with increasing BaO content. It is interesting to note here that these two δ_{iso} values are comparable to those reported [10] for the corner-shared Q_4^4 in α-TeO_2 (~1469 ppm) and edge-shared Q_4^4 in β-TeO_2 (~1569 ppm). Therefore, it is tempting to assign these two peaks in $(BaO)_x(TeO_2)_{100-x}$ glasses to corner- and edge-sharing Q_4^4 species, respectively. If this structural assignment is correct then the compositional variation of their relative fractions (Fig. 5, Table 1) suggests that the initial depolymerization of the Te-O-Te network by the incorporation of BaO affects the corner-sharing species somewhat more than the edge-sharing species.

Finally, an interesting and unique situation arises in Fig. 7 for the |Δ| and η values near δ_{iso} ~1600 ppm, where the |Δ| values remain near those characteristic of the Q_4^4 species while the η values decrease to those characteristic of the Q_3^m species (Fig. 8). Such combination of |Δ| and η values has been reported for two of the four Te sites in a low-temperature polymorph of $Na_2Te_4O_9$, while those for the other two Te sites were reported to be characteristic of typical Q_4^4 species [7]. Recently the structure of this polymorph has been solved using single crystal X-ray diffraction which indicated that the 2 Te sites in this polymorph are indeed of the type Q_4^4 while the other 2 Te are present as Q_4^3 species [20]. Therefore, we argue that the Q_4^3 sites are characterized by this unusual combination of |Δ| and η values and assign the corresponding peak at 1600 ppm in the glass spectra to the Q_4^3 species. When taken together, the compositional variation of the relative fractions of various Q species in Fig. 5 then indicates that addition of BaO primarily results in the depolymerization of the Te-O-Te network via replacement of the charge-neutral corner and the edge-sharing Q_4^4 species primarily with the negatively charged Q_4^3 and Q_3^1 species (Fig. 5). In contrast, and in spite of its appearance upon the initial addition of BaO at 5 mol% level, the relative fraction of the charge-neutral Q_3^2 species, changes rather little with further addition of BaO up to 25 mol% (Fig. 5). This evolution of the Q-speciation is qualitatively similar to that proposed for Li- and Na-tellurite glasses in a previous study based on combined X-ray and neutron diffraction and

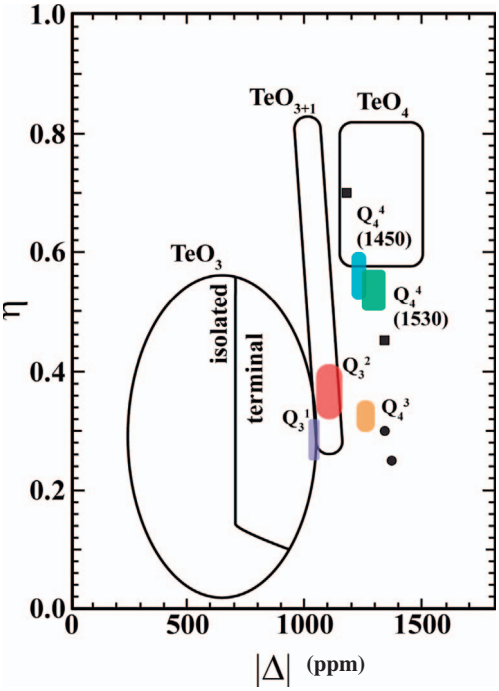

Fig. 8. $|\Delta|$ vs. η map of Sakida et al. [10] showing the range of $|\Delta|$ and η values for the five Q species in BaO-TeO_2 glasses at their respective peak positions, as determined in this study (see Table 1). The black squares and black circles denote the Q_4^4 and Q_4^3 environments, respectively, in $Na_2Te_4O_9$ crystal, as reported in [7].

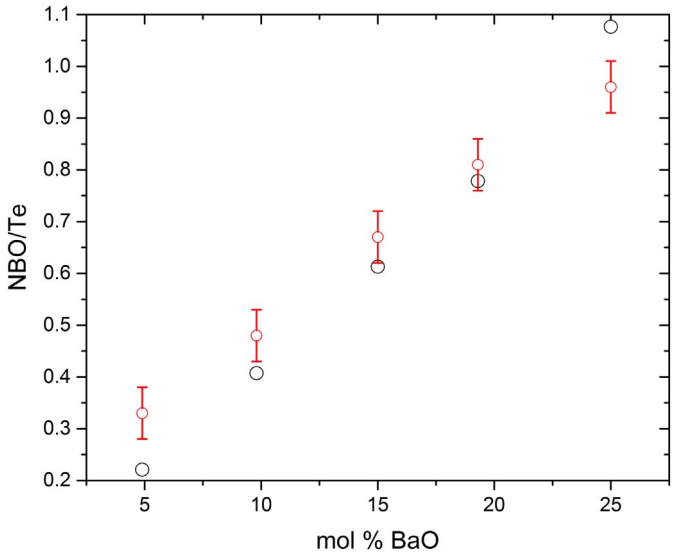

Fig. 9. Comparison between calculated (black symbols) and experimentally determined (red symbols) NBO/Te for various BaO-TeO_2 glasses. See text for details. (For interpretation of the references to color in this figure legend, the reader is referred to the web version of this article.)

Reverse Monte Carlo simulation [3]. This study also noted the preferential increase in the relative concentration of charged Q species (Q_4^3, Q_3^1 and Q_3^0) in alkali tellurite glasses with increasing degree of network modification.

The Q-speciation, thus obtained from the simulation of the isotropic ^{125}Te NMR spectra, can now be used to calculate the composition dependence of the NBO concentration in these glasses. Ideally, this NBO concentration would be the same as that expected from the chemical composition if one considers that the addition of every mole of alkali or alkaline-earth oxide creates 2 moles of NBO in oxide glasses where the coordination number of the network forming cation (e.g. Si^{4+}, P^{5+}) remains constant, irrespective of glass composition. However, as it is apparent from the ^{125}Te NMR data presented here and is also widely accepted in the literature, addition of modifying alkali or alkaline-earth oxides to TeO_2 results in a progressive conversion of TeO_4 bipyramids to TeO_3 pyramids. Therefore, in addition to the NBOs created by the addition of the modifier oxide, one also needs to consider the NBOs created by the reaction: $TeO_4 \rightarrow TeO_3$ + NBO. The extent of this $TeO_4 \rightarrow TeO_3$ conversion in tellurites cannot be predicted a priori and has been shown in alkali tellurites to depend on the nature of the alkali ion. Therefore, here we use the total relative fraction of all the three-fold-coordinated Te atoms $f(Q_3^m)$ as obtained from the ^{125}Te NMR line shape analysis (Table 1 and Fig. 5) to estimate the total NBO per Te cation in each of the $(BaO)_x(TeO_2)_{100-x}$ glasses using the relation: $NBO/Te = [2x/(100-x)] + f(Q_3^m)$; where x is the mol% modifier alkali or alkaline-earth oxide. The validity of this relation can be readily checked for any tellurite crystal with known Q-speciation. For example, the $K_2Te_4O_9$ crystal contains equal fractions of Q_4^3 and Q_3^2 species each of which contain 1 NBO and hence, NBO/Te = 1.0 [9]. On the other hand, using the above equation with $x = 20$ and $f(Q_3^m) = 0.5$, for $K_2Te_4O_9$ one also obtains NBO/Te = 1.0. Similarly, for the $Cs_2Te_2O_5$ crystal [9], which contains only Q_3^1 species (i.e., 2 NBO), NBO/Te = 2.0 which is also the result if one uses $x = 33.33$ and $f(Q_3^m) = 1.0$ in the above relation. The comparison between the NBO/Te values obtained from the total Q-speciation in Table 1 and those calculated from the glass composition (x = mol% BaO) in combination with $f(Q_3^m)$ from Table 1 is shown in Fig. 9. The good agreement between these NBO/Te values provides key support for the structural assignment of the ^{125}Te NMR peaks proposed in this study and suggest that two-dimensional ^{125}Te isotropic-anisotropic chemical shift correlation NMR spectroscopy could be a viable technique for investigating the chemical evolution of the highly complex network structure of tellurite glasses.

4. Conclusions

The complex structural evolution of BaO-TeO_2 glasses is studied using high-resolution ^{125}Te *pj*MATPASS/CPMG NMR spectroscopy. It is shown that structural assignment of various ^{125}Te resonances may require the consideration of the full chemical shift tensor, rather than just the isotropic shift. TeO_2-rich glasses and possibly glassy TeO_2 itself is characterized by a network of corner and edge-shared Q_4^4 units. Progressive addition of BaO results in a modification of this network and a decrease in its connectivity as the concentration of NBO increases monotonically via replacement of the charge-neutral Q_4^4 units, predominantly with the negatively charged Q_4^3 and Q_3^1 units. Finally, we would like to emphasize that the future applications of such 2D NMR spectroscopic techniques as MATPASS, that provide information on the correlation of the isotropic and anisotropic chemical shifts, can be combined with density functional theory based calculations to obtain robust structural models of glasses with complex coordination chemistry.

Acknowledgements

This work was supported by a grant from the National Science Foundation (NSF-DMR 1505185) to SS. The National High Magnetic Field Laboratory is supported through the National Science Foundation Cooperative Agreement (DMR-1157490) and by the State of Florida. The authors wish to thank Mr. Nicholas Botto for assistance with the electron probe microanalyses.

References

[1] R. El-Mallawany, Tellurite Glasses Handbook: Physical Properties and Data, Second edition, CRC Press, Boca Raton, FL, 2012.
[2] F. Mazurier, M. Levy, J.L. Souquet, J. Phys. IV France 02 (1992) C2185–C2188.

[3] J.C. McLaughlin, S.L. Tagg, J.W. Zwanziger, J. Phys. Chem. B 105 (2001) 67–75.
[4] S. Neov, S. Ishmaev, V. Kozhukharov, J. Non-Cryst. Solids 192&193 (1995) 61.
[5] S. Sakida, S. Hayakawab, T. Yokoa, J. Non-Cryst. Solids 243 (1999) 13.
[6] E.R. Barney, A.C. Hannon, D. Holland, N. Umesaki, M. Tatsumisago, R.G. Orman, S. Feller, J. Phys. Chem. Lett. 4 (2013) 2312.
[7] D. Holland, J. Bailey, G. Ward, B. Turner, P. Tierney, R. Dupree, Solid State Nucl. Magn. Reson. 27 (2005) 16–27.
[8] E.R. Barney, A.C. Hannon, D. Holland, N. Umesaki, M. Tatsumisago, J. Non-Cryst. Solids 414 (2015) 33–41.
[9] C.R. Becker, S.L. Lagg, J.C. Huffman, J.W. Zwanziger, Inorg. Chem. 36 (1997) 5559–5564.
[10] S. Sakida, S. Hayakawab, T. Yokoa, J. Non-Cryst. Solids 243 (1999) 1–12.
[11] S.L. Tagg, J.C. Huffman, J.W. Zwanziger, Chem. Mater. 6 (1994) 1884–1889.
[12] D.C. Kaseman, I. Hung, K. Lee, K. Kovnir, Z. Gan, B. Aitken, S. Sen, J. Phys. Chem. B 119 (2015) 2081–2088.
[13] I. Hung, T. Edwards, S. Sen, Z. Gan, J. Magn. Reson. 221 (2012) 103–109.
[14] D.C. Kaseman, I. Hung, Z. Gan, B. Aitken, S. Currie, S. Sen, J. Phys. Chem. B 118 (2014) 2284–2293.
[15] I. Hung, L. Zhou, F. Pourpoint, C.P. Grey, Z. Gan, J. Am. Chem. Soc. 134 (2012) 1898–1901.
[16] R.K. Harris, E.D. Becker, S.M.C. De Menezes, R. Goodfellow, P. Granger, Pure Appl. Chem. 73 (2001) 1795–1818.
[17] D. Massiot, F. Fayon, M. Capron, I. King, S.L. Calvé, B. Alonso, J.O. Durand, B. Bujoli, Z. Gan, G. Hoatson, Magn. Reson. Chem. 40 (2002) 70–76.
[18] E.R. Shaaban, Y.B. Saddeek, M.A. Rafea, Philos. Mag. 89 (1) (2009) 27–39.
[19] N. Mochida, K. Takahashi, K. Nakata, S. Shibusawa, J. Ceram. Assoc. Jpn 86 (1979) 317–326.
[20] D.W. Lee, K.M. Ok, Inorg. Chem. 53 (2014) 10642–10648.